

Coverage Characterization of STAR-RIS Networks: NOMA and OMA

Chenyu Wu, Yuanwei Liu, *Senior Member, IEEE*, Xidong Mu, *Graduate Student Member, IEEE*, Xuemai Gu, *Member, IEEE*, Octavia A. Dobre, *Fellow, IEEE*

Abstract—The novel concept of simultaneously transmitting and reflecting reconfigurable intelligent surface (STAR-RIS) is investigated, where incident signals can be transmitted and reflected to users located at different sides of the surface. In particular, the fundamental coverage range of STAR-RIS aided two-user communication networks is studied. A sum coverage range maximization problem is formulated for both non-orthogonal multiple access (NOMA) and orthogonal multiple access (OMA), where the resource allocation at the access point and the transmission and reflection coefficients at the STAR-RIS are jointly optimized to satisfy the communication requirements of users. For NOMA, we transform the non-convex decoding order constraint into a linear constraint and the resulting problem is convex, which can be optimally solved. For OMA, we first show that the optimization problem for given time/frequency resource allocation is convex. Then, we employ the one dimensional search-based algorithm to obtain the optimal solution. Numerical results reveal that the coverage can be significantly extended by the STAR-RIS compared with conventional RISs.

Index Terms—Reconfigurable intelligent surface, simultaneous transmission and reflection, non-orthogonal multiple access, coverage range, resource allocation

I. INTRODUCTION

Reconfigurable intelligent surfaces (RISs) have been envisioned as a revolutionary technology to enhance the spectrum efficiency (SE) and to improve the coverage range for beyond fifth-generation (5G) wireless communication networks [1], [2]. An RIS is composed of massive low-cost and programmable elements, and thus, can reconfigure the propagation of incident wireless signals by adjusting the amplitudes and phase shifts of each element. Due to the nearly passive working mode, RISs can enhance the communication performance without the need of radio frequency (RF) chains compared with active relaying, which reduces the energy consumption and the hardware costs [3]. Moreover, when the direct link between the access point (AP) and users is blocked, RIS can be deployed to provide additional signal paths, thus satisfying the basic communication requirements of users in the signal dead zone. Driven by the above advantages, RISs have received extensive interests from both industry

and academy to fully exploit its benefits. The adoption and superiority of RISs for communication networks have been studied in previous works [4]–[8], where the joint beamforming optimization and the energy efficiency analysis have been investigated. However, these contributions mainly focus on RISs which act as reflective metasurfaces; hence, the served users ought to be on the same side of RIS, i.e. *half-space coverage*, which limits the flexibility of deploying RISs.

To overcome this drawback, recently, a novel concept of simultaneous transmitting and reflecting RISs (STAR-RISs) has been proposed [9], [10]. Different from existing reflecting-only RISs, STAR-RISs can simultaneously transmit and reflect the incident signals. Hence, *full-space coverage* can be enabled. STAR-RISs provide new degree-of-freedom for manipulating signal propagation, thus increasing the flexibility for network design. Despite the above appealing characteristics, to the best of our knowledge, the superiority of STAR-RISs in terms of coverage range has not been studied yet, which motivates this work.

In this article, we aim to characterize the fundamental coverage range of STAR-RIS aided communication networks. In particular, an AP communicates with one transmitted user (T user) and one reflected user (R user) employing both non-orthogonal multiple access (NOMA) and orthogonal multiple access (OMA) with the aid of an STAR-RIS. A sum coverage range maximization problem for the joint optimization of the resource allocation at the AP and the transmission and reflecting coefficients at the STAR-RIS is formulated for each multiple access scheme, subject to the quality-of-service (QoS) requirements of users. Specifically, for NOMA, we convert the joint optimization problem into a convex one by transforming the non-convex decoding order constraint. For OMA, we present a convex subproblem with given time/frequency resource allocation and then employ the one dimensional search-based algorithm to obtain the optimal solution. Numerical results unveil that the coverage range of STAR-RISs is significantly enhanced by NOMA. Moreover, compared with conventional RIS, STAR-RIS can greatly extend the network coverage range for both NOMA and OMA.

The remainder of this article is organized as follows. The system model and problem formulation are presented in Section II. Efficient algorithms are designed to solve problems for NOMA and OMA in Section III. In Section IV, numerical results are presented to verify the effectiveness of STAR-RISs. Finally, Section V concludes this article.

C. Wu, and X. Gu are with the School of Electronic and Information Engineering, Harbin Institute of Technology (HIT), Harbin, 150001, China. (e-mail: {wuchenyu, guxuemail}@hit.edu.cn).

Y. Liu is with the School of Electronic Engineering and Computer Science, Queen Mary University of London, London E1 4NS, UK, (email: yuanwei.liu@qmul.ac.uk).

X. Mu is with School of Artificial Intelligence, Beijing University of Posts and Telecommunications, Beijing, 100876, China (email: muxidong@bupt.edu.cn).

O. A. Dobre is with the Department of Electrical and Computer Engineering, Memorial University, St. John's, NL A1C 5S7, Canada (e-mail: odobre@mun.ca).

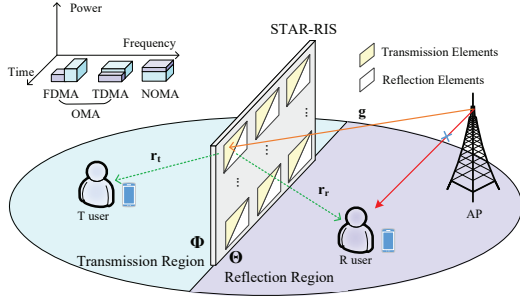


Fig. 1. Illustration of an STAR-RIS aided two-user downlink communication systems employing NOMA and OMA.

II. SYSTEM MODEL AND PROBLEM FORMULATION

A. System Model

We consider a narrow-band STAR-RIS aided downlink communication network operating over frequency-flat channels, where a single-antenna AP communicates with two single-antenna users with the aid of an STAR-RIS consisting of M elements. As illustrated in Fig. 1, the T user is located behind the STAR-RIS (i.e., transmission region), while the R user is located in front of the STAR-RIS (i.e., reflection region). We assume that the direct communication links between the AP and the two users are blocked by obstacles. Let $\mathbf{r}_k \in \mathbb{C}^{M \times 1}$ denote the channel between STAR-RIS and user $k \in \mathcal{K} = \{t, r\}$, which is modeled as the following Rician fading channel:

$$\mathbf{r}_k = \sqrt{\frac{\rho_0}{D_k^{\alpha_{RU}}}} \underbrace{\left(\sqrt{\frac{K_{RU}}{K_{RU} + 1}} \mathbf{r}_k^{\text{LoS}} + \sqrt{\frac{1}{K_{RU} + 1}} \mathbf{r}_k^{\text{NLoS}} \right)}_{\bar{\mathbf{r}}_k}, \quad (1)$$

where D_k denotes the distance between the STAR-RIS and user k , $\alpha_{RU} \geq 2$ denotes the path loss exponent, ρ_0 represents the path loss at a reference distance of 1 meter, $\mathbf{r}_k^{\text{LoS}} \in \mathbb{C}^{M \times 1}$ and $\mathbf{r}_k^{\text{NLoS}} \in \mathbb{C}^{M \times 1}$ are the deterministic line-of-sight (LoS) component of the array response and the random non-line-of-sight (NLoS) component modeled as Rayleigh fading, respectively. K_{RU} denotes the Rician factor. For simplicity, we use $\bar{\mathbf{r}}_k$ to represent the summed terms of $\mathbf{r}_k^{\text{LoS}}$ and $\mathbf{r}_k^{\text{NLoS}}$.

Similarly, the Rician fading channel of the AP-STAR-RIS link, denoted by $\mathbf{g} \in \mathbb{C}^{M \times 1}$ is expressed as:

$$\mathbf{g} = \sqrt{\frac{\rho_0}{d^{\alpha_{AR}}}} \left(\sqrt{\frac{K_{AR}}{K_{AR} + 1}} \mathbf{g}^{\text{LoS}} + \sqrt{\frac{1}{K_{AR} + 1}} \mathbf{g}^{\text{NLoS}} \right), \quad (2)$$

where $\mathbf{g}^{\text{LoS}} \in \mathbb{C}^{M \times 1}$ and $\mathbf{g}^{\text{NLoS}} \in \mathbb{C}^{M \times 1}$ are the LoS and NLoS components, respectively. d is the distance between AP and STAR-RIS, α_{AR} and K_{AR} are path loss exponent and Rician factor, respectively.

B. STAR-RIS Model

Different from existing works [4]–[8], each STAR-RIS element can simultaneously operate in two modes, namely transmission and reflection [9], [10]. For transmission, the STAR-RIS allows the incident signal to pass through it via

reconfiguring the signal propagation to the T user. For reflection, the RIS reflects and reconfigures the incident signal propagation to the R user. In order to reduce the overhead for information exchange between the AP and the STAR-RIS, we assume that all elements have the same amplitude coefficients. Specifically, let $\Theta_t = \sqrt{\beta_t} \text{diag}(e^{j\theta_1^t}, e^{j\theta_2^t}, \dots, e^{j\theta_M^t})$ and $\Theta_r = \sqrt{\beta_r} \text{diag}(e^{j\theta_1^r}, e^{j\theta_2^r}, \dots, e^{j\theta_M^r})$ denote the STAR-RIS transmission-coefficient and reflection-coefficient matrices, respectively. In particular, $\sqrt{\beta_t}, \sqrt{\beta_r} \in [0, 1]$ and $\theta_m^t, \theta_m^r \in [0, 2\pi], m \in \mathcal{M} = \{1, \dots, M\}$ characterize the amplitude and phase shift adjustments imposed on the incident signals facilitated by the m th element during transmission and reflection, respectively. Note that due to the law of energy conservation, the sum energy of the transmitted and reflected signals has to be equal to that of the incident signals [9], [10]; then, we have $\beta_r + \beta_t = 1$.

Further, the effective channel power gain of user k is given by

$$|h_k|^2 = |\mathbf{r}_k^H \Theta_k \mathbf{g}|^2 = \frac{\rho_0 \beta_k}{D_k^{\alpha_{RU}}} |\mathbf{q}_k \mathbf{v}_k|^2, \quad (3)$$

where $\mathbf{q}_k = \bar{\mathbf{r}}_k^H \text{diag}(\mathbf{g}) = \{q_{m,k}, m = 1, \dots, M, \forall k\}$ and $\mathbf{v}_k \triangleq [e^{j\theta_1^k}, e^{j\theta_2^k}, \dots, e^{j\theta_M^k}]^T$ is defined as phase shift vectors for transmission and reflection. Let p_k denote the transmit power allocated to user k . In the following, we consider NOMA and OMA transmission schemes.

C. Multiple Access Schemes

1) *NOMA*: For NOMA, the AP transmits the superposition coded signals of the two users throughout the same time and frequency resources. Let s_k denote the transmitted signal for user k from the AP and $\mathbb{E}[|s_k|^2] = 1$. The received signal at user k is given as follows:

$$y_k = (\mathbf{r}_k^H \Theta_k \mathbf{g}) (\sqrt{p_t} s_t + \sqrt{p_r} s_r) + n_k, \quad (4)$$

where $n_k \sim \mathcal{CN}(0, \sigma^2)$ denotes the additive white Gaussian noise at user k with variance σ^2 . Let the binary variable $\lambda(k) \in \{0, 1\}$ denote the decoding order of user k , which satisfies $\lambda(t) + \lambda(r) = 1$. For instance, if the T user is the strong user with higher channel power gain (i.e., $|h_t|^2 \geq |h_r|^2$), which first decodes the signal of R user before decoding its own signal, i.e., through successive interference cancellation (SIC), we have $\lambda(t) = 1$ and $\lambda(r) = 0$. Otherwise, $\lambda(t) = 0$ and $\lambda(r) = 1$ [11]. Therefore, the achievable communication rate of user k for NOMA is given by

$$r_k^N = \log_2 \left(1 + \frac{\rho_0 p_k \beta_k |\mathbf{q}_k \mathbf{v}_k|^2}{\lambda(\bar{k}) \rho_0 p_{\bar{k}} \beta_{\bar{k}} |\mathbf{q}_{\bar{k}} \mathbf{v}_{\bar{k}}|^2 + D_k^{\alpha_{RU}} \sigma^2} \right), \quad (5)$$

where \bar{k} represents the other user.

2) *OMA*: For OMA, we consider the general case where the AP transmits the signals of the two users throughout the orthogonal frequency/time resources which can be allocated adaptively [12]. Let $\omega_k \in [0, 1]$ denote the proportion of resource blocks allocated to user k . Then, the achievable rate

of user k for OMA can be expressed as

$$r_k^O = \omega_k \log_2 \left(1 + \frac{\rho_0 p_k \beta_k |\mathbf{q}_k \mathbf{v}_k|^2}{\omega_k D_k^{\alpha_{RU}} \sigma^2} \right). \quad (6)$$

D. Problem Formulation

In this article, we aim to characterize the coverage range of STAR-RIS for NOMA and OMA, subject to the predefined QoS requirements of users. Let D_0 denote the maximum coverage range provided by STAR-RIS, which is the sum of the transmission coverage range, D_t , and the reflection coverage range, D_r . Moreover, let μ_k denote the coverage allocation factor for user k , where user k can be served successfully within the maximum distance $\mu_k D_0$. We have $\mu_k \geq 0$ and $\mu_t + \mu_r = 1$. A larger value of μ_k means a higher priority of user k . Then, the characterization of the coverage range of the STAR-RIS for NOMA can be formulated as the following optimization problem:

$$\max_{\{p_k, \beta_k, D_k, \lambda(k), \mathbf{v}_k, D_0\}} D_0 \quad (7a)$$

$$\text{s.t. } D_k \geq u_k D_0, \forall k \in \mathcal{K}, \quad (7b)$$

$$D_k \geq 1, \forall k \in \mathcal{K}, \quad (7c)$$

$$r_k^N \geq \gamma_k, \forall k \in \mathcal{K}, \quad (7d)$$

$$\sum_k p_k \leq P_{\max}, \quad (7e)$$

$$\theta_m^k \in [0, 2\pi], \forall m \in \mathcal{M}, k \in \mathcal{K}, \quad (7f)$$

$$\beta_r + \beta_t = 1, \quad (7g)$$

$$\lambda(k) \in \{0, 1\}, \lambda(t) + \lambda(r) = 1, \quad (7h)$$

$$\begin{cases} |h_t|^2 \geq |h_r|^2, & \text{if } \lambda(t) = 1 \\ |h_t|^2 \leq |h_r|^2, & \text{otherwise} \end{cases}, \quad (7i)$$

where (7c) ensures that the users locate at the far-field region for STAR-RIS; (7d) denotes the QoS requirements of users; (7e) denotes the total power constraint; (7f) is the phase shift constraint for each element of STAR-RIS; (7g) represents the energy conservation constraint; (7h) and (7i) are the decoding order constraints for SIC.

For OMA, the optimization problem can be formulated as follows:

$$\max_{\{p_k, \beta_k, \omega_k, D_k, \mathbf{v}_k, D_0\}} D_0 \quad (8a)$$

$$\text{s.t. } r_k^O \geq \gamma_k, \forall k \in \mathcal{K}, \quad (8b)$$

$$\sum_k \omega_k \leq 1, \quad (8c)$$

$$(7b), (7c), (7e) - (7g). \quad (8d)$$

The main challenges for solving the two problems are as follows: Firstly, the introduced transmission and reflection coefficients of the STAR-RIS are coupled with the variables of network resource allocation, which increases the complexity of the optimization problems. Secondly, for NOMA, the decoding order constraint for SIC has to be effectively tackled since it is non-convex.

Remark 1. For the two-user multiple access scenario with STAR-RIS, \mathbf{v}_k can be maximized independently by combining signals from different paths coherently.

It is noted that with STAR-RIS, the phase shift vectors \mathbf{v}_k for the two sides can be optimized independently. In the two user scenario, since the achievable rate monotonically increases with $|\mathbf{q}_k \mathbf{v}_k|$, we can simply maximize them by adjusting the incident signals to have the same phases. Then, we denote $c_k = \max_{\mathbf{v}_k} |\mathbf{q}_k \mathbf{v}_k|^2 = \sum_{m=1}^M (|q_{m,k}|^2)$.

III. PROPOSED SOLUTIONS

A. NOMA Case

The problem for NOMA case is complex due to the binary decoding order (7h) and non-convex constraint (7i) for SIC. To handle these difficulties, we present the following lemma:

Lemma 1. The non-convex constraint (7i) for SIC can be transformed into linear one related to reflection coefficient β_k and rate requirement γ_k .

Proof. We take $\lambda(r) = 1$ as an example and give the Lagrangian function $\mathcal{L}_1(\mathbf{y}, \boldsymbol{\mu}, \lambda, v)$ which is shown in (9), where $\mathbf{y} = \{p_k, \beta_k, D_k, D_0, \forall k\}$ denotes the variable set. The Karush-Kuhn-Tucker (KKT) conditions are listed as follows:

$$\nabla_{\beta_k^*} \mathcal{L}_1 = (2^{\gamma_k} - 1) \mu_k \frac{(D_k^*)^\alpha}{(\beta_k^*)^2 c_k} - \lambda = 0, \quad (10a)$$

$$\nabla_{p_k^*} \mathcal{L}_1 = v - \mu_1 = 0, \quad (10b)$$

$$\nabla_{p_r^*} \mathcal{L}_1 = (2^{\gamma_t} - 1) \mu_1 - \mu_2 + v = 0, \quad (10c)$$

where E denotes the terms which are independent of β_k and p_k , $\boldsymbol{\mu} = [\mu_1, \mu_2], v, \lambda$ are non-negative Lagrangian multipliers. Then, we have $(\frac{\beta_r^*}{\beta_t^*})^2 = \frac{2^{\gamma_t}(2^{\gamma_r}-1)}{2^{\gamma_t}-1} (\frac{D_r}{D_t})^\alpha \frac{a}{b}$. Then $|h_t|^2 \leq |h_r|^2 \Leftrightarrow \frac{\beta_t a}{D_t^\alpha} \geq \frac{\beta_r b}{D_r^\alpha} \Leftrightarrow \beta_r \leq \frac{2^{\gamma_t}(2^{\gamma_r}-1)}{2^{\gamma_t}-1} \beta_t$. Following the similar derivation, for the decoding order $\lambda(t) = 1$, the non-convex constraint for SIC $|h_t|^2 \geq |h_r|^2$ is equivalent to $\beta_t \leq \frac{2^{\gamma_r}(2^{\gamma_t}-1)}{2^{\gamma_r}-1} \beta_r$, which is a linear one.

The relaxed problem for a given decoding order is convex, which can be proved by the following lemma:

Lemma 2. For $x, y > 0$ and $\alpha \geq 2$, $f(x, y) = \frac{y^\alpha}{x}$ is a convex function with respect to x and y .

Proof. When $x, y > 0$ and $\alpha \geq 2$, it is easy to get $\frac{\partial^2 f}{\partial x^2} \cdot \frac{\partial^2 f}{\partial y^2} - (\frac{\partial^2 f}{\partial x \partial y})^2 = (\alpha^2 - 2\alpha)y^{2\alpha-2}x^{-4} \geq 0$ and $\frac{\partial^2 f}{\partial x^2} = 2y^\alpha x^{-3} \geq 0$; then, the Hessian matrix of function $f(x, y)$ is positive semidefinite. Thus, $f(x, y)$ is convex.

We also take the decoding order $\lambda(r) = 1$ as an example and rewrite the QoS requirement constraint (7d). Then, the transformed problem for NOMA is given by:

$$\max_{\{p_k, \beta_k, D_k, D_0\}} D_0 \quad (11a)$$

$$(2^{\gamma_t} - 1) \left(a \frac{D_t^{\alpha_{RU}}}{\beta_t} + p_r \right) \leq p_t, \quad (11b)$$

$$(2^{\gamma_r} - 1) b \frac{D_r^{\alpha_{RU}}}{\beta_r} \leq p_r, \quad (11c)$$

$$\beta_r \leq \frac{2^{\gamma_t}(2^{\gamma_r}-1)}{2^{\gamma_t}-1} \beta_t, \quad (11d)$$

$$\mathcal{L}_1(\mathbf{y}, \boldsymbol{\mu}, \lambda, v) = v \left(\sum_k p_k - P_{\max} \right) + \lambda \left(\sum_k \beta_k - 1 \right) + \mu_1 \left[(2^{\gamma_t} - 1) \left(a \frac{D_t^{\alpha_{RU}}}{\beta_t} + p_r \right) - p_t \right] + \mu_2 b \left[(2^{\gamma_r} - 1) \frac{D_r^{\alpha_{RU}}}{\beta_r} - p_r \right] + E. \quad (9)$$

$$(7b), (7c), (7e), (7g). \quad (11e)$$

where $a = \frac{\sigma^2}{\rho_0 c_t}$ and $b = \frac{\sigma^2}{\rho_0 c_r}$ are constants with respect to environmental parameters and phase shifts. Based on **Lemma 2**, it is observed that problem (11) is convex. For NOMA, the coverage characterization problem (7) can be solved by exhaustively searching over 2 decoding orders. The coverage range is then given by $D_0^* = \arg \max_{k \in \mathcal{K}} (D_{0(\lambda(k)=1)}^*)$. The computational complexity of solving the NOMA problem is given by $\mathcal{O}(2N_1^{3.5})$ [13], where $N_1 = 7$ is the number of variables.

B. OMA Case

Before solving the problem, we first have the following lemma, which reveals the relation between optimal amplitude coefficient and power allocation.

Lemma 3. For the case OMA, the optimal power allocation p_k^* and amplitude coefficient β_k^* satisfy $\frac{p_t^*}{\beta_t^*} = \frac{p_r^*}{\beta_r^*} = P_{\max}$.

Proof. The Lagrangian function of the problem is given by

$$\mathcal{L}_2(\mathbf{x}, \boldsymbol{\mu}, \lambda, v) = \mu_k \left[\omega_k \log_2 \left(1 + \frac{\rho_0 p_k \beta_k c_k}{\omega_k D_k^{\alpha_{RU}} \sigma^2} \right) - \gamma_k \right] + v(p_t + p_r - P_{\max}) + \lambda(\beta_t + \beta_r - 1) + E, \quad (12)$$

where $\mathbf{x} = \{p_k, \beta_k, D_k, \omega_k, D_0, \forall k\}$ is the variable set, E denotes the terms which are independent of β_k and p_k , $\boldsymbol{\mu} = [\mu_1, \mu_2]$, v are non-negative Lagrangian multipliers, and λ is multiplier regarding the equality constraint. Since the KKT conditions are necessary for all local optimal points, we have $\nabla_{p_k^*} \mathcal{L}_2 = 0$ and $\nabla_{\beta_k^*} \mathcal{L}_2 = 0$ which are expressed as:

$$\nabla_{\beta_k^*} \mathcal{L}_2 = -\log_2(e) \mu_k \omega_k^* \frac{a p_k^*}{1 + a p_k^* \beta_k^*} + v = 0, \quad (13a)$$

$$\nabla_{p_k^*} \mathcal{L}_2 = -\log_2(e) \mu_k \omega_k^* \frac{a \beta_k^*}{1 + a p_k^* \beta_k^*} + \lambda = 0, \quad (13b)$$

where $a = \frac{\rho_0 c_t}{\omega_t^* (D_t^*)^{\alpha} \sigma^2}$, $b = \frac{\rho_0 c_r}{\omega_r^* (D_r^*)^{\alpha} \sigma^2}$, and $\alpha = \alpha_{RU}$. With (13), we get $\frac{p_t^*}{\beta_t^*} = \frac{p_r^*}{\beta_r^*} = \frac{v}{\lambda}$. It is easy to deduce that $v > 0$ for $\gamma_k > 0$. With the complementary slackness conditions $v(p_t^* + p_r^* - P_{\max}) = 0$, constraint (7e) is active and can be met with equality. The linear relation of p_k^* and β_k^* is proved and the ratio between them is P_{\max} . **Lemma 3** gives us an interesting insight to reduce the number of optimization variables. Furthermore, based on **Lemma 2** and **Lemma 3**, we find that with fixed time/bandwidth allocation $\omega_k = \omega_0$, the subproblem for OMA is convex, which is expressed as:

$$\max_{\{\beta_k, D_k, D_0\}} D_0 \quad (14a)$$

$$\frac{\omega_0 (2^{\frac{\gamma_k}{\omega_0}} - 1) \sigma^2}{\rho_0 c_k} \frac{D_k^{\alpha_{RU}}}{\beta_k} - P_{\max} \beta_k \leq 0, \quad (14b)$$

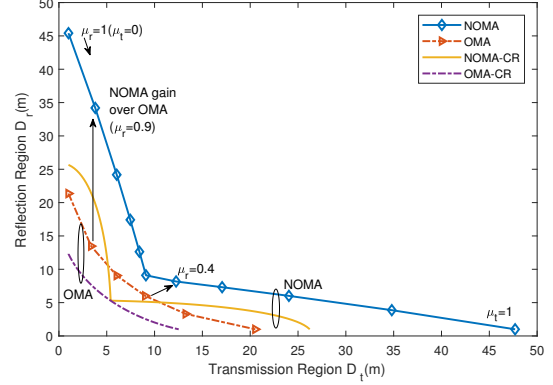


Fig. 2. The coverage range D_t and D_r with QoS requirements $\gamma_k = 5$ bps/Hz, where "CR" refers to conventional RISs.

$$(7b), (7c), (7g). \quad (14c)$$

Problem (14) is a convex optimization problem, which can be solved efficiently by solvers like CVX [14]. Thus, the optimal solution for problem (8) can be obtained using the one-dimensional search over $0 \leq \omega_k \leq 1$. The computational complexity of solving the OMA problem is given by $\mathcal{O}(N_2^{3.5} \log_2(1/\epsilon))$ [13], where $N_2 = 5$ is the number of variables and ϵ is the accuracy for one-dimensional search.

IV. SIMULATION RESULTS

In this section, we provide numerical results to validate the effectiveness of our proposed designs. We consider a two-dimensional coordinate system, where the STAR-RIS is equipped with $M = 100$ elements. The AP is located at the origin, while the STAR-RIS is located at (50,0) meters. We set $\rho_0 = -30$ dB, $\sigma^2 = -80$ dBm, $\alpha_{RU} = \alpha_{AR} = 2.2$, $K_{RU} = K_{AR} = 10$, $P_{\max} = 30$ dBm.

For performance comparison, we consider conventional RISs (CR) as a benchmark scheme. In particular, we employ one reflecting-only RIS and one transmitting-only RIS, each consisting of $M/2$ elements to achieve full-space coverage for a fair comparison with the STAR-RIS.

In Fig. 2, we characterize the coverage range of the STAR-RIS with different coverage range allocation factors μ_k . We set the QoS requirements as $\gamma_k = 5$ bps/Hz and plot the coverage range pairs (D_t, D_r) . By varying μ_k , we get different tuples of the optimal coverage range for the transmission region and reflection region. It is observed that for NOMA, the performance gain in terms of coverage range is not prominent for homogenous priority, i.e., μ_t and μ_r are close. The performance gain of NOMA over OMA is more pronounced as μ_k approaches 0 or 1, since the multiplexing gain of the time/frequency resource is more remarkable. It is also observed that by deploying the STAR-RIS, the coverage range is nearly doubled for both NOMA and OMA compared with

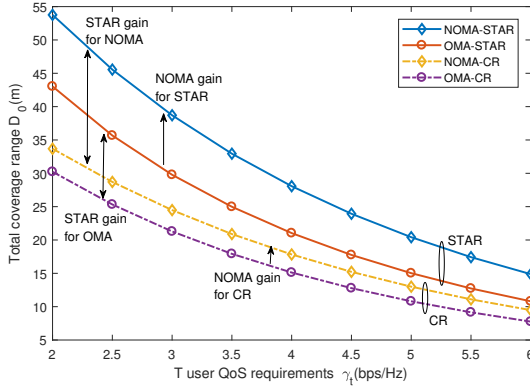


Fig. 3. The total coverage range D_0 versus different γ_t , with fixed R user QoS requirements $\gamma_r = 5$ bps/Hz.

that of conventional RISs, which verifies the effectiveness of the proposed STAR-RIS.

In Fig. 3, we depict the total coverage range, D_0 , versus different T user's QoS requirement, γ_t . We fix the R user's QoS requirements as $\gamma_r = 5$ bps/Hz and the coverage allocation factor $\mu_t = 0.6$. As seen from Fig. 3, for conventional RISs, the performance gap between NOMA and OMA is negligible. However, for STAR-RIS, NOMA achieves a significant performance gain in terms of coverage range compared with OMA, i.e., *NOMA gain*. This is because the simultaneously transmitting and reflecting scheme can enlarge the channel disparity between the two users, where NOMA yields higher performance gain than OMA. Furthermore, the STAR-RIS provides a significant performance gain for both NOMA and OMA compared with conventional RIS, i.e., *STAR gain*. The results also confirm the superiority of the proposed STAR-RIS.

In Fig. 4, we plot the coverage range of the T user, D_t , versus the number of elements, M . The QoS requirements are set to $\gamma_k = 3$ bps/Hz and the coverage allocation factor is $\mu_t = 0.6$. It can be observed that the coverage range increases linearly as there are larger total number of elements for all cases. The STAR gain over conventional RISs is more pronounced as M increases. Meanwhile, NOMA can also enhance the network performance of both STAR-RISs and conventional RISs for asymmetric channels, i.e., μ_t is not close to μ_r . It can be seen from Fig. 4 that the NOMA gain for STAR-RISs is larger than that for conventional RISs. The results indicate that the combination of NOMA and STAR-RIS is a win-win strategy.

V. CONCLUSIONS

In this article, we studied the fundamental coverage characterization of STAR-RIS assisted two-user communication networks. A sum coverage range maximization problem for NOMA and OMA was formulated, which involved a joint optimization of the transmission and reflection coefficients at the STAR-RIS and resource allocation at the AP. For NOMA, we transformed the non-convex constraints to make the problem convex. For OMA, we used the one-dimensional search based algorithm to find the optimal solution. Simulation results showed that the STAR-RIS provided wider coverage

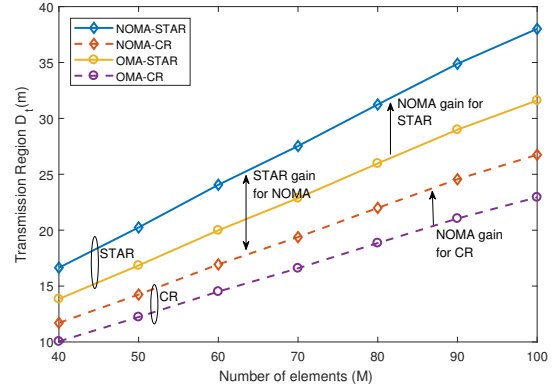


Fig. 4. The coverage range D_t versus different number of total elements, with QoS requirements $\gamma_k = 3$ bps/Hz.

range compared with conventional reflecting and transmitting-only RIS. Furthermore, the interplay between STAR-RIS and NOMA increased the flexibility for network design.

REFERENCES

- [1] M. Di Renzo *et al.*, "Smart radio environments empowered by reconfigurable intelligent surfaces: How it works, state of research, and the road ahead," *IEEE J. Sel. Areas Commun.*, vol. 38, pp. 2450–2525, Nov. 2020.
- [2] Y. Liu *et al.*, "Reconfigurable intelligent surfaces: Principles and opportunities," *IEEE Commun. Surv. Tut.*, accepted, 2021.
- [3] E. Basar *et al.*, "Wireless communications through reconfigurable intelligent surfaces," *IEEE Access*, vol. 7, pp. 116753–116773, 2019.
- [4] Q. Wu and R. Zhang, "Intelligent reflecting surface enhanced wireless network via joint active and passive beamforming," *IEEE Trans. Wireless Commun.*, vol. 18, pp. 5394–5409, Nov. 2019.
- [5] X. Mu, Y. Liu, L. Guo, J. Lin, and N. Al-Dhahir, "Exploiting intelligent reflecting surfaces in NOMA networks: Joint beamforming optimization," *IEEE Trans. Wireless Commun.*, vol. 19, pp. 6884–6898, Oct. 2020.
- [6] C. Huang, A. Zappone, G. C. Alexandropoulos, M. Debbah, and C. Yuen, "Reconfigurable intelligent surfaces for energy efficiency in wireless communication," *IEEE Trans. Wireless Commun.*, vol. 18, pp. 4157–4170, Aug. 2019.
- [7] M. Zeng, X. Li, G. Li, W. Hao, and O. A. Dobre, "Sum rate maximization for IRS-assisted uplink NOMA," *IEEE Commun. Lett.*, vol. 25, pp. 234–238, Jan. 2021.
- [8] F. E. Bouanani, S. Muhaidat, P. C. Sofotasios, O. A. Dobre, and O. S. Badarneh, "Performance analysis of intelligent reflecting surface aided wireless networks with wireless power transfer," *IEEE Commun. Lett.*, vol. 25, pp. 793–797, Mar. 2021.
- [9] J. Xu *et al.*, "STAR-RISs: Simultaneous transmitting and reflecting reconfigurable intelligent surfaces." [Online]. Available: <https://arxiv.org/abs/2101.09663>.
- [10] Y. Liu *et al.*, "STAR: Simultaneous transmission and reflection for 360° coverage by intelligent surfaces." [Online]. Available: <https://arxiv.org/abs/2103.09104>.
- [11] X. Mu, Y. Liu, L. Guo, J. Lin, and N. Al-Dhahir, "Capacity and optimal resource allocation for IRS-assisted multi-user communication systems," *IEEE Trans. Commun.*, Early Access, 2021, doi:10.1109/TCOMM.2021.3062651.
- [12] Z. Chen, Z. Ding, X. Dai, and R. Zhang, "An optimization perspective of the superiority of NOMA compared to conventional OMA," *IEEE Trans. Signal Process.*, vol. 65, pp. 5191–5202, Oct. 2017.
- [13] S. Boyd and L. Vandenberghe, *Convex Optimization*. Cambridge, U.K.: Cambridge Univ. Press, 2004.
- [14] M. Grant and S. Boyd, "CVX: Matlab software for disciplined convex programming." [Online]. Available: <http://cvxr.com/cvx>, 2014.